EMERGING FACES IN ANISOTROPICALLY ETCHED CRYSTALS

Carlo H. Séquin

Computer Science Division, EECS Department
University of California, Berkeley, CA 94720

ABSTRACT

The behavior of anisotropically etched crystalline materials is studied at the geometrical level. The crystal shape is represented with a polyhedral boundary description in which the various faces advance with rates solely dependent on their orientations. Particular attention is paid to the situations under which new truncation or bevel faces that were not previously present appear at vertices or edges of the crystal. A new method of analysis based on convex hulls over the extrema of the inverse of the etch-rate polar diagram (slowness diagram) is presented which can handle corners of arbitrary complexity. Results are presented that were obtained with a prototype of a 3-dimensional etching simulator based on this representation.

1. INTRODUCTION

For certain anisotropic etching solutions such as KOH (potassium hydroxide in water) or EDP (a watery solution of ethylenediamine and pyrocatechol), the dense {1 1 1} planes of a silicon crystal which have face normals with components of equal magnitude in the x, y, and z directions, will etch a hundred times more slowly than other, more loosely packed planes [Bass78, Bean78]. This fact has been used for making ultra flat faces, vertical walls, tapered pits, gratings, or beveled cantilevers [Pete82]. Figure 1 shows how ink-jet nozzles can be fabricated as a combination of pyramids on one side of the wafer with properly aligned etch pits cut through from the other side. This structure relies on the slowness of the etching of the {1 1 1} planes to define the tapered walls on the inside and outside of the pyramids.

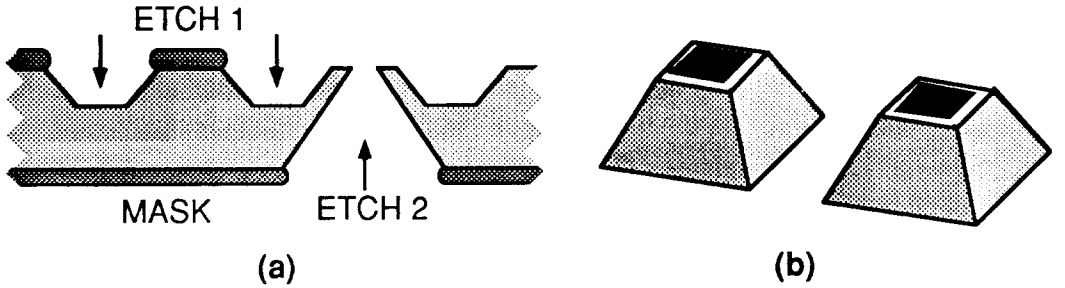

Figure 1: *Construction (a) and final shape (b) of inkjet nozzles produced with anisotropic etching.*

Under other circumstances, much more complex geometries can result from such anisotropic etching. When several different faces and edges come together at odd angles, it is often difficult to predict and to visualize what geometries might result. Tools are needed that can properly model such etching processes in order to fully exploit the potential for tailoring silicon and other substances to form sophisticated transducers or micro-electromechanical systems. Ideally such process simulation tools are as fast and interactive as possible. This goal excludes simulation by stochastic cell removal in an array of "atomic" cells. It requires that the etching processes be modeled at some higher level of abstraction. For efficiency and simulation speed, one would thus like to model the facets of the crystal surface as entities that can be advanced and modified as a whole.

In this paper we investigate the macroscopic geometrical effects that describe the etching of anisotropic but uniform crystalline materials. In particular we study the shape changes that occur because of the advancement of differently oriented faces at different speeds. We present some new insights into the geometrical changes that can occur, such as the emergence of new faces at edges and corners. We then outline an approach to construct an efficient simulator that makes such geometric effects visible. Our prototype simulator for anisotropic etching is based on a boundary representation of the current surface of the crystal and modifies this description as a function of etching time.

2. GEOMETRY OF ANISOTROPIC ETCHING

2.1 Etch-Rate Diagram

Anisotropic etching relies on the fact that in all crystalline structures the atomic bonds in some planes are more exposed than in some others. A suitably designed etching agent will thus attack and strip away certain plane orientations more quickly than others. Throughout this paper we will assume the presence of a homogeneous crystalline material with a constant orientation of its lattice. As a consequence, during etching, a planar face will remain planar and move parallel to itself at some rate that depends only on the orientation of the face [Fran58]. These etch-rates, measured normal to the actual crystal surface, are described conveniently in a polar plot in which the distance from the origin to the polar plot *surface* (or *curve* in 2D) indicates the etch-rate for that particular normal direction (Fig.2a). Figure 2b shows a complete polar plot for a hypothetical two-dimensional biclinic crystal.

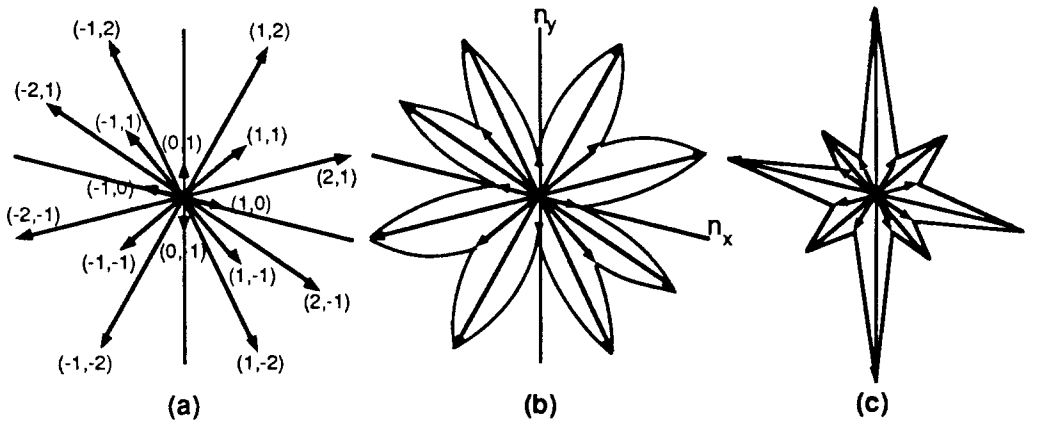

Figure 2: *Some key etch rates (a), the complete etch-rate diagram (b), and its inverse: the slowness diagram (c).*

For the analysis of how the etching process alters the geometry of the crystal surface, it is more informative to plot the reciprocal value of the etch-rate; this results in a *slowness diagram* (Fig.2c). In this inside-out mirroring, short vectors in one figure turn into long ones in the other, and vice versa. Notice that in this inversion process the contour of the slowness diagram takes on a shape that is nearly piecewise linear; we have used this fact to simplify the construction of usable 3-dimensional etch-rate polar diagrams [Séqu91].

2.2 Offset Surface Construction

For didactical reasons, we first present our approach to modeling the etching process with a two-dimensional model. The extension to three dimensions is then conceptually straight-forward — even though much harder to implement. If the complete polar diagram (2π in 2D, 4π in 3D) is known, then constructing the new crystal shape after some specified etching time amounts to computing an offset surface with proper, orientation-dependent offsets. Every face is advanced by a distance proportional to the etch-rate in

that particular direction. These faces are then intersected, thus determining the new positions of the edges and corners.

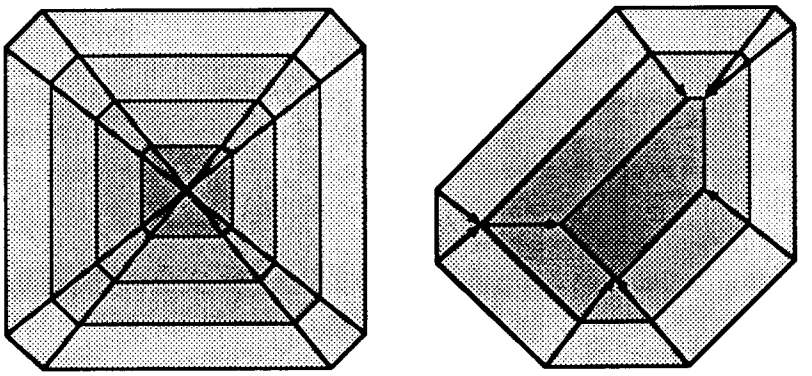

Figure 3: *Snapshots in time of etching contours: special case where all vertex trajectories meet in one point (a), the general case with disappearing faces (b).*

Under the above circumstances, it is known that vertices between faces as well as small surface elements of a given orientation move through space on linear trajectories [Fran58, BMFS73]. However, the crystal shape will not simply change in scale as in the special case shown in Figure 3a. Depending on the angles and sizes of the starting faces, some faces may disappear quickly while others become dominant (Fig.3b). The real difficulty stems from the fact that **new** faces can emerge from vertices with orientations that were not previously present. At convex corners, faces of high etch-rates may suddenly appear, while in concave corners, bevel faces may be produced by the slow-etching faces. Faces of equivalent orientation do not **always** appear – it depends on the geometry of the corner and, in particular, on the orientation of the adjacent faces. For instance, in Figure 4, a diagonal facet will emerge at the upper left corner, but not at the upper right one. To understand this, we have to look at the vertex movements in more detail.

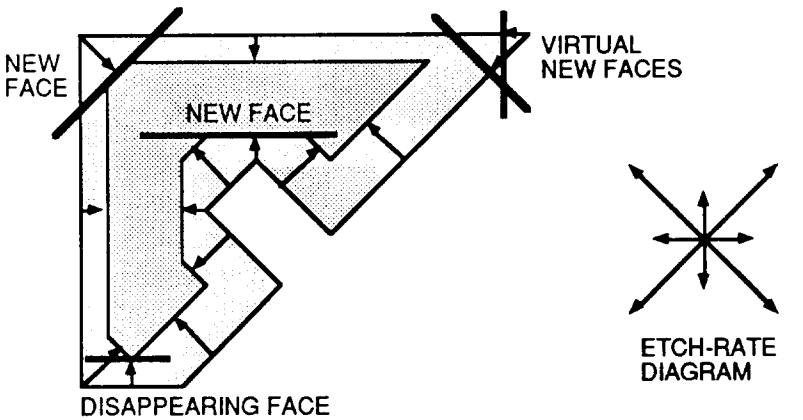

Figure 4: *Offset contours with disappearing and with newly emerging faces.*

2.3 Vertex Movements

Consider the simple two-dimensional crystals shown in Figures 3 and 4. Any two faces forming a corner get advanced by their respective etch-rates, and the new corner location is formed by the intersection of the new face positions. From the vertex' locations at two different etching times, its trajectory can readily be determined. However, there is a more elegant way to derive this vertex movement directly. The vertex slowness vector is the perpendicular vector onto the chord connecting the two slowness vectors of the two adjacent faces [Fran58].

This fact is easily proven with Figure 5 for either concave or convex corners. The circle c_{ab} with etch-rate vector r_c as its diameter acts as a circle of Thales for the two right-angled triangles involving the etch-rates r_a and r_b and their corresponding crystal surface etching fronts. If this circle c_{ab} is inverted at the unit circle c_u around the original vertex position, it will transform into a straight line L_{ab}. This line forms the chord between the tips of the two slowness vectors S_a and S_b which have resulted from the inversion of the two etch-rate vectors r_a and r_b. The slowness vector S_{ab} of the vertex motion is the inverse of the vector r_c. Because of the symmetric position of the latter in the circle c_{ab}, S_{ab} is also perpendicular to the chordal line L_{ab}.

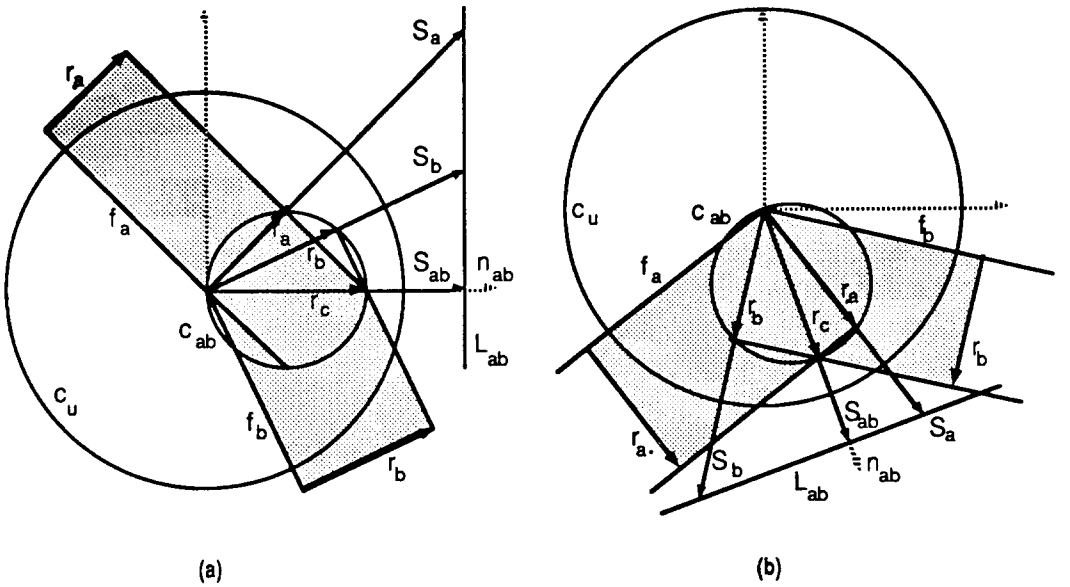

Figure 5: *Proof that vertex moves normal to chord between slowness vectors: concave 2D case (a) and convex 2D corner (b).*

2.4 Growing and Shrinking Faces

Knowing how the vertices move as a function of time, permits us also to construct the various facets between them. As long as the vertex trajectories do not intersect, the number of faces will not change, even though their sizes will change as a function of time. If the vertex trajectories converge, the face will shrink and will eventually disappear; if the trajectories diverge, the face will actually grow in size, – possibly at the expense of one or both of its neighbors.

Knowing the trajectories of all vertices allows us to parameterize the etched crystal surface in time and forms the basis for an interactive display of the whole etching process on a particular piece of crystal geometry. Since all expressions are linear functions of time, the vertex positions and thus the coordinates that define all the faces that make up the crystal surface can readily be evaluated in real-time as the surface is displayed on a computer graphics screen. However, we need to pre-calculate key frames at "interesting" time points when the structure of the crystal surface changes, such as when adjacent vertices merge, and the edge between them disappears. But in between such time points, we can simply display all faces after the parameter substitution for the current time has been made.

To build a truly useful simulator, we also must test for non-local interactions where a vertex trajectory intersects with some unrelated face. The latter issue becomes important if we etch long enough so that holes may etch to the other side of the wafer or overhanging features may get cut off. Dealing with such non-local, topological changes presents an additional set of difficulties since it requires more than just strictly local analysis. We will come back to this issue later.

3. CORNER ANALYSIS IN 2 D

3.1 Emerging New Faces

If the etch-rate diagram shows significant speed differences, the situation can get even more complicated: Faces cannot only disappear, but new faces with orientations not previously seen can emerge along edges or at corners. Such a case is illustrated in Figure 6a, where face f_c is growing at the expense of its two neighbors. Extrapolating the vertex trajectories backwards, shows that such a face can even emerge out of a simple vertex between two faces f_a and f_b (Fig.6b). The main difficulty here is that it is not *a priori* clear what face orientations should be considered for potential emergence of new faces at a particular corner.

Just considering the original two faces f_a and f_b in Figure 6b, the vertex between them would move in the direction S_{ab}, perpendicular to the chord between the tips of S_a and S_b. But if there is a face orientation f_c between f_a and f_b that moves **faster** than the combined action of the two faces f_a and f_b on the vertex, the new face will become visible at this vertex. Such a face orientation will readily manifest itself in the slowness diagram as a slowness vector that does not extend all the way to the chord. This will cause an **inward** bump S_c in the slowness curve (which, of course, also passes through S_a and S_b). In this case, the original vertex will split. Two new vertices V_{ac} and V_{ab}, moving perpendicular to the two sub-chords, i.e., along S_{ac} and S_{cb}, will drift apart as a function of time and form the new face f_c between them.

Similarly, it can be seen that for concave corners, the **slowest** etch directions will lead to **outward** bumps in the slowness curve which then produce new vertices that move apart and form new faces between them (Fig.6c).

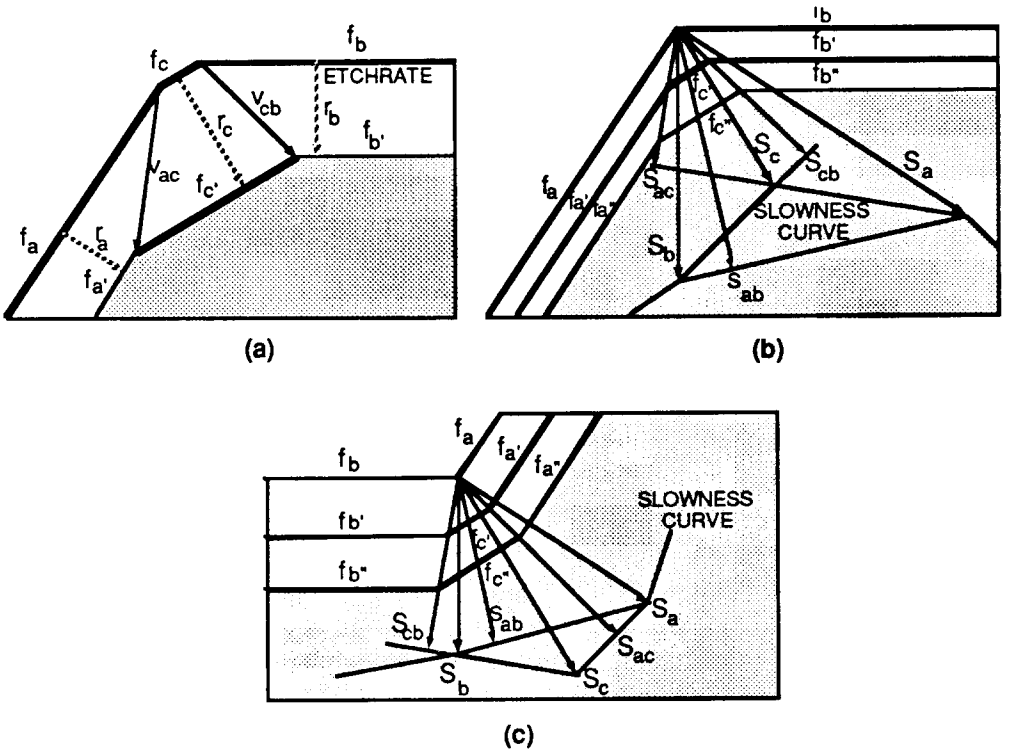

Figure 6: *Growing face (a) and development of a new face due to a minimum in the slowness curve (b) and due to a maximum (c).*

Moreover, under the right circumstances, e.g., isotropic etching of concave corners, rounded features can develop, which means that an infinity of new face orientations are introduced. Thus, in general, one must analyze the complete polar diagram to find all orientations in which new faces can potentially form. Whether a particular face will actually appear at a specific corner, is then a question of what angles it forms with the adjacent two faces.

In three dimensions this problem can become particularly challenging since multiple new bevel faces may emerge along individual edges which then interact in complicated ways with additional faces that truncate the corner where they all merge. A robust and reliable technique is required that can handle all possible situations.

3.2 Convex Hull Constructions

The general case of a concave 2D corner with an arbitrary, ragged etch-rate or slowness diagram is shown in Figure 7a. In this case there are several locally dominant slow-etching faces which all might lead to visible faces, and they would all have to be analyzed in their local environment of the adjacent faces. This analysis can be done in a global manner by finding the convex hull over all the bumps generated by local maxima in the slowness curve. The corners in this convex hull correspond to all the truncation faces that will become visible at this vertex. Similarly, at a **convex** crystal corner, the hull over the **minima** of the slowness curve defines all the newly emerging **fast**-etching faces (Fig.7b).

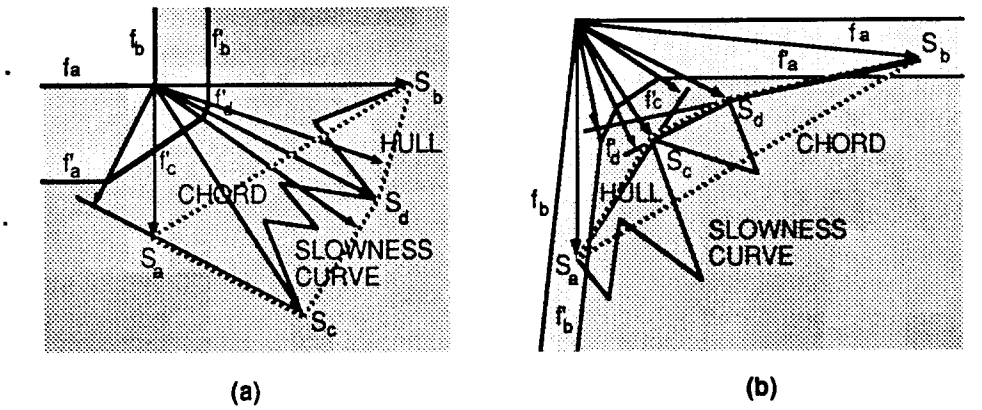

Figure 7: *Convex hull construction to find new faces: at a concave 2D corner (a), and at a convex 2D corner (b).*

In cases, where the slowness curve has noticeable curvature — as in the case of uniform etching where it is a circle — this curvature may give rise to an infinite set of new growing face orientations, i.e. it will lead to a rounded piece of crystal geometry. For simplicity and efficiency, this round shape is approximated in a piece-wise linear manner with a polygon with enough facets to provide the accuracy needed in the etching simulation.

At this point it should be emphasized that it is not strictly the fastest-etching face orientations that produce the emerging facets at a convex crystal vertex — it depends on the local constellation. Data published by Sato *et. al.* [SaKT89] provides an interesting case in point. They look at the emerging bevel faces at an edge between two {100} type planes when etching in aqueous KOH. In a separate experiment they had determined that at higher temperatures (78°C) the {320} planes show the fastest etch-rate. Experimentally they observe two bevel faces with angles of 34° from the {100} planes (Fig.8a) — as one would expect from analyzing the corresponding slowness diagram (Fig.8a).

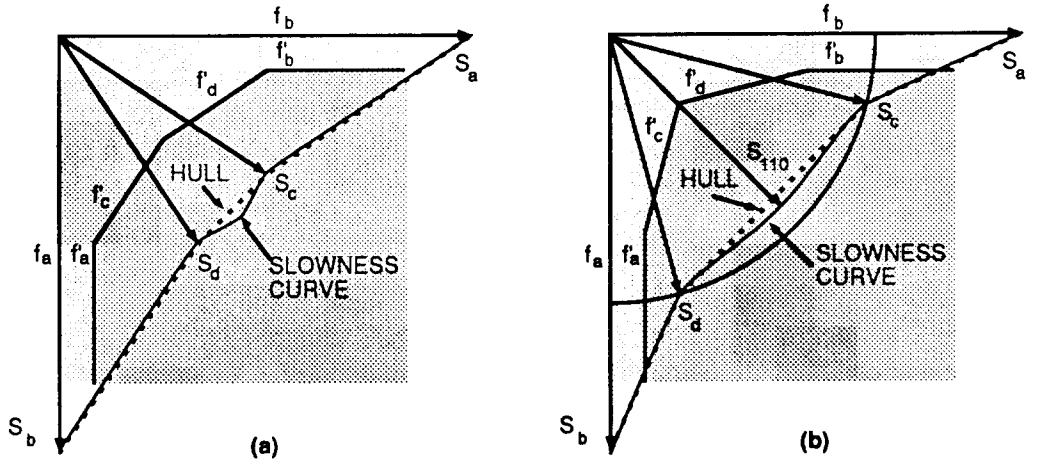

Figure 8: *The usual situation where the fastest etching directions yields the emerging bevel faces (a) and a special situation where the marginally faster face is suppressed by the compound effect by its two neighbors (b).*

At lower temperatures (40°C) the maximum of the etch-rate moves towards the {110} direction, and for low enough temperatures one might thus expect to see a 45° bevel appearing at this edge. But they still observed a double bevel corresponding to two faces with angles of 16° from the {100} planes (Fig.8b). Drawing the slowness diagram for this situation reveals that even though the S_{110} is the shortest vector in this diagram, it is long enough to cross the cord between the two instances of slowness vectors S_c and S_d that point towards two inward kinks of the slowness curve; thus S_{110} does **not** form a corner in the convex hull around the slowness curve. In such tricky situations, the convex hull analysis automatically predicts the right result.

3.3 Need for Vertex Analysis

At the start of an etching simulation, we need to check all the corners to determine the possible presence of virtual faces that will grow into existence. But once the vertices have been analyzed and their (possibly split) vertex trajectories have been calculated, no further analysis on these same vertices is needed until the surface structure changes. When the two trajectories of two adjacent vertices intersect, the vertices merge and the edge between them disappears. A new situation is created with a vertex between two faces that now span a potentially larger range of angles between them (Fig.9a). How much analysis does this new situation require ? Figure 9a implies that there cannot emerge any new face orientations that would not have already shown themselves before the merger: Any slowness vector that might give rise to a new face, e.g. S_{21}, would have to fall inside the chord L_{ac}; however, such a vector would also stop short of the chords L_{ab} and L_{bc} and would thus lead to a new face even before the vertex merger. On the other hand, if we look at the situation shown in Figure 9b where a convex vertex merges with a concave one, it is possible to have a slowness vector, e.g. S_{10}, that crosses the original chord L_{bc} but stops short of the chord L_{ac} formed by the vertex merger, thus producing a new face after the merger.

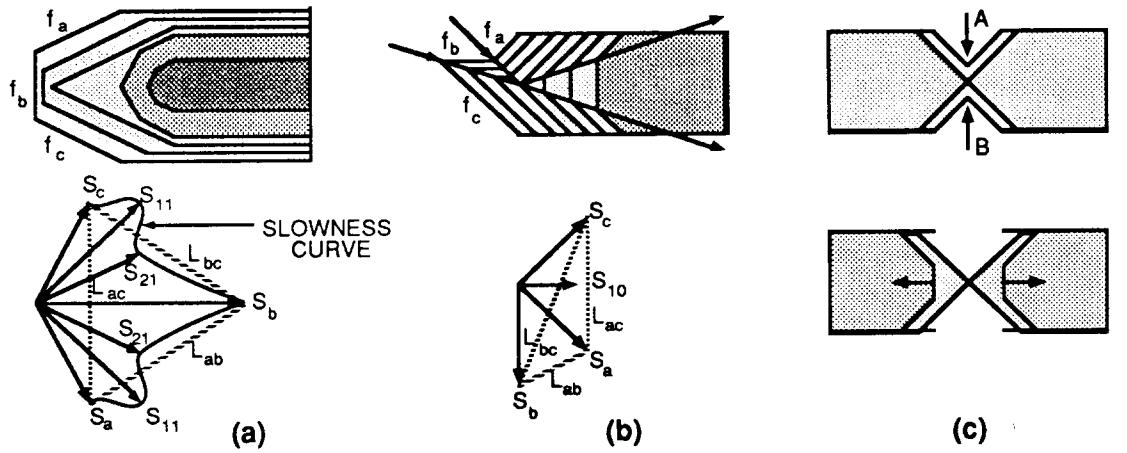

Figure 9: *When do merging vertices provide a need for a new vertex analysis ? Merging convex vertices (a), merging convex and concave vertex (b), topological change of contour (c).*

Furthermore, whenever there is a merger of non-adjacent vertices, such as A and B in Figure 9c, or the crash of a vertex into another face, we obtain a new topological situation

that needs to be analyzed from scratch. For simplicity and to be on the safe side, our simulator repeats the vertex analysis after every merger and any time the surface structure changes.

4. ETCHING SIMULATIONS IN 2D

4.1 Simulator Prototype

A two-dimensional simulator was first developed as a learning experience. The simulator accepts etch-rate values for certain key directions and then calculates several intermediate etch-rates by mixing the etch-rates of the adjacent key directions in the proper proportions [Foote 89]. This creates a quasi-smooth piecewise linear polar diagram. The specific etch-rate required for a particular face orientation is then obtained from this data base by interpolation.

The simulator then reads in a polygonal starting shape in UniGrafix format [SéSm90]. The vertex analysis is carried out for all original vertices, and the newly emerging faces are introduced into the contour data structure where necessary. The corresponding vertex trajectories are calculated at the same time. This yields a parameterized description of the complete etching contour as a function of time.

For this two-dimensional prototype, non-local interactions are searched for in a brute-force manner. All vertex trajectories are intersected with one another and with all existing faces. The corresponding intersection events are inserted into a time-ordered event list which marks the times when there are changes in the contour structure. The simulator then runs from event to event until it stops at a user-specified time.

4.2 Etching Contours in 2D

Figure 10a shows a result of etching a rectangular shape of a two-dimensional crystal with an assumed underlying biclinic slowness curve as indicated in Figure 10b. The eight faces of type {2 1} etch fastest and will dominate a convex shape after some etching time. Superposed on Figure 10a are the paths taken by the various vertices, showing clearly the splitting and merging of vertices and the corresponding appearance and disappearance of faces.

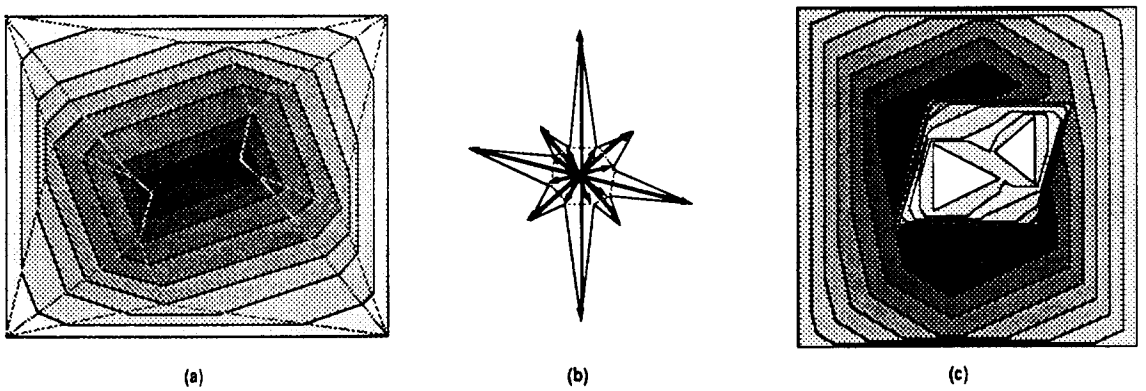

Figure 10: *Nested etching contours on a hypothetical 2D crystal (a), underlying biclinic slowness diagram (b), merging contours causing topology changes (c).*

A more complicated case for a similar type of crystalline material is depicted in Figure 10c. Here the starting geometry has two triangular holes. As etching progresses, these holes first merge with each other, later with the outer contour.

5. TOOLS FOR 3D ANALYSIS

Our three-dimensional etching simulator takes the same basic approach as the 2D simulator above. The main difference is that there are now many more different key directions, and the interpolation to determine the etch-rate in an arbitrary direction becomes more difficult. Also, the data structures in 3D are more complicated and are harder to implement.

The analysis of three-dimensional corners is more difficult, because they can be of several different types. There are not just convex and concave corners to be distinguished. There are also saddle corners that are neither one nor the other type. Furthermore, while a polygon corner has exactly two sides attached, a polyhedral corner may have an unlimited number of faces incident.

Nevertheless, the analysis that has to be performed at three-dimensional corners is conceptually the same as in the planar case. We need to find the extrema on the proper hull over the slowness surface segment (SSS) within the solid angle defined by the face normals around the vertex of interest. These extrema define the new faces that will emerge at this vertex or on the associated edges. These faces must be properly inserted into the data structures describing the boundary surface and then advanced according to their own etch-rates. The added difficulty is that there may be emerging bevel faces along the edges in addition to new truncation faces at the corner, which then all interact with one another. We will deal with these issues one at a time. In all cases, the discussion gets facilitated by looking at the *vertex figure* projected onto the slowness surface.

5.1 Slowness Surface in 3D

As in two dimensions, the analysis of what happens to three-dimensional crystal corners is most conveniently carried out with the help of the slowness diagram. Now this inverse of the etch-rate diagram is a 4π polar diagram that contains the necessary information for all possible directions. Unfortunately, complete etch-rate information for all directions can rarely be found in the literature; typically just two-dimensional slices through this surface are published, sometimes enhanced with a few specific measurements for some of the more interesting, low-order crystal plane orientations. Our first task is therefore to construct a complete and consistent slowness diagram.

First, etch-rates are entered for the key directions in which extreme values can be expected, enhanced with additional intermediate directions based on available data and on the desired accuracy of the etching simulations. Around this skeleton, the complete slowness surface is then approximated with a triangulated polyhedron that uses the given values as corners. This linearized approximation seems justified for most interesting cases with large variations of the etch-rate, since we observed in our studies on 2D crystals that the resulting slowness curves were often piecewise linear [Foot90, p21].

For example in a simple cubic lattice one might only specify the etch-rates for the six key orientations {1 0 0}, {1 1 0}, {1 1 1}, {2 1 0}, {2 1 1}, and {2 2 1}. In this case, the slowness diagram has 98 vertices and 192 triangular faces. The stereographic projection of half of this surface is shown in Figure 11a.

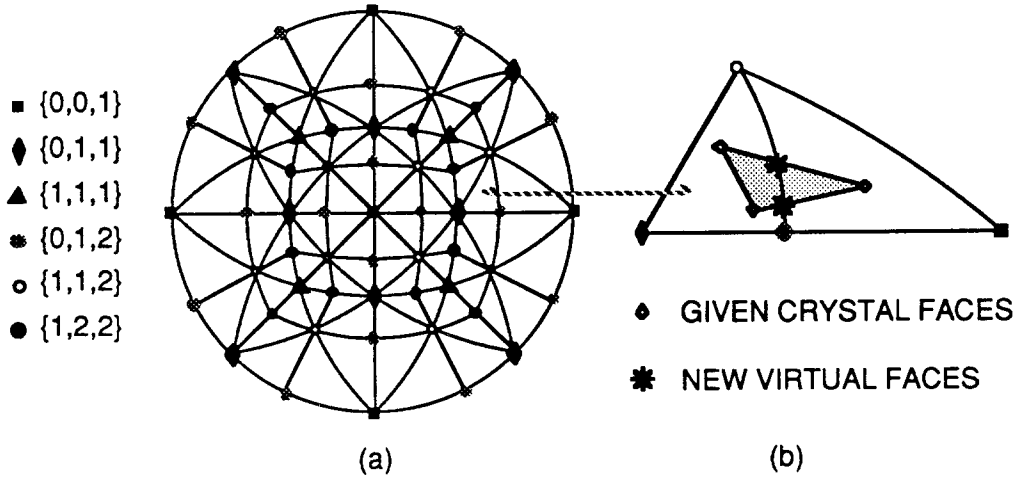

Figure 11: *Stereographic projection of key directions in a simple cubic lattice (a) and superposition of a vertex diagram of a simple crystal corner (b).*

To model the behavior of a **silicon** lattice, it might be more appropriate to replace the key orientations {2 2 1} with {3 3 1} and to include the orientations {3 2 0} explicitly, since there is evidence that under certain circumstances, maxima of the etch-rate can occur in these directions [SeCs82] [SaKT89].

The above data structure can now be queried. Slowness vectors for specific orientations are extracted by barycentric interpolation in one of the triangular facets shown in Figure 11. In this linear model, new corner truncation faces can only appear at the vertices, and new edge bevels only at orientations that correspond to points on the edges of this polyhedral slowness diagram (Fig.11b). This makes the computation of the convex hull over portions of the slowness surface simple and renders the analysis of the edge-connectivity changes at 3D corners manageable.

5.2 Vertex Figures

As a reference for the relevant face orientations and directions at a crystal corner, it is useful to draw its *vertex figure*. This is done by intersecting the normal vectors for all faces incident on this corner with the unit sphere. In this paper we draw the face normals **into** the crystal bulk, so that the normals and the etch-rate vectors point in the same direction. Adjacent faces sharing a common edge are then connected by great circle arcs in the vertex diagram, and this arc is labeled convex or concave (typically shown dashed) according to the dihedral angle at the corresponding crystal edge. For a vertex formed by N faces (Figs.12a,d: N=4), the vertex diagram will form an N-sided contour (Fig.12b) which may be self-intersecting if there is a mix of convex and concave edges coming together at that vertex (Fig.12e). If we label the faces around the crystal corner a, b, c,... in counter-clockwise order (CCW) as seen from the outside of the crystal and compare the

resulting orientation of the vertex figure, we find that for true convex or concave corners the positive (CCW) orientation is maintained, whereas for saddle points the orientation is reversed – either in the whole vertex figure, or at least in some part of it if the vertex figure is self-intersecting.

This vertex figure is then superposed onto the unit-sphere projection of the slowness diagram (Fig.12b,e). The inside of this diagram represents the SSS that needs to be analyzed for extrema that might lead to newly emerging faces. It should be noted that the straight lines in Figure 12 b,e are really images of great arcs on a sphere.

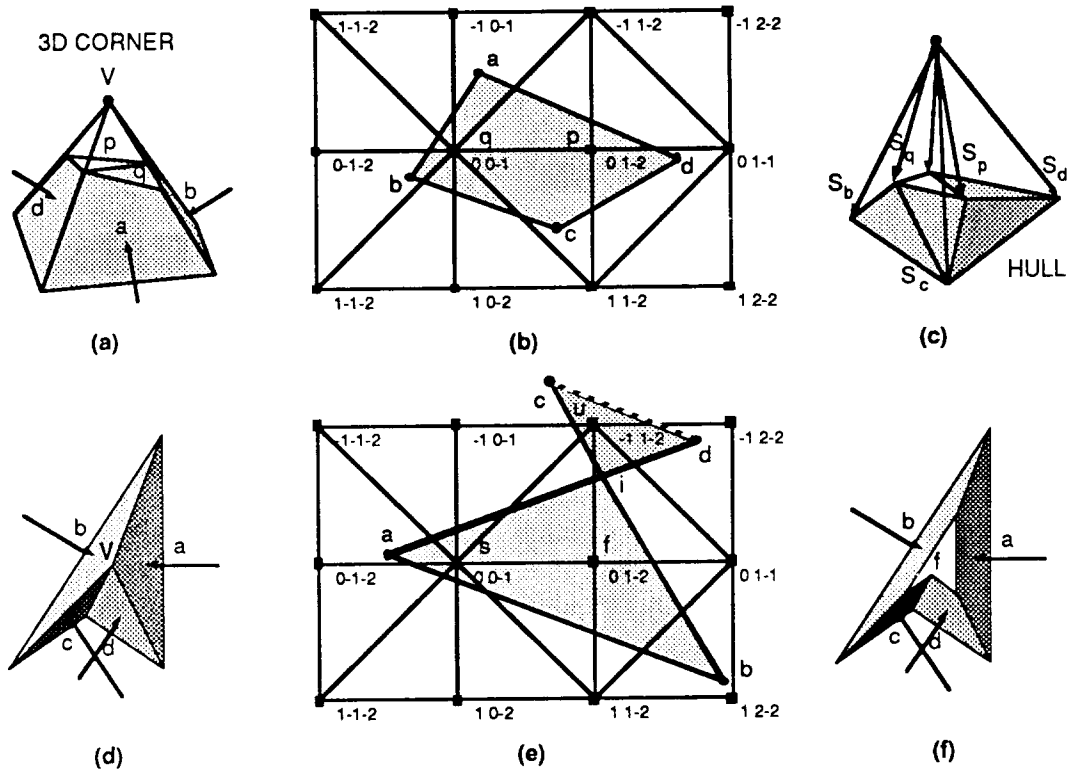

Figure 12: *Crystal corner (a), vertex figure (b), and convex slowness hull (c). Another crystal corner (d), its vertex figure (e), and the truncated result (f).*

6. EDGE ANALYSIS

The analysis of the evolving new crystal geometry starts with the edges. The arcs between two points in the vertex figure denoting the orientations of two adjacent faces represent all orientations perpendicular to the crystal edge between the two faces. If the slowness surface is cut along such an arc, one obtains a slowness curve like the ones analyzed in the first half of this paper. Depending on whether the crystal edge is convex or concave, one has to select the extrema on either the inner or the outer hull of the slowness curve. If extrema of the right sign are present, the edge will split into two or more parallel edges with bevel faces in between. Since we now assume that the slowness surface is polyhedral, we can expect extrema of the slowness curve to occur only at points where the arcs of the vertex figure cross the edges (ridges or grooves) of the slowness polyhedron.

Each edge can split into several bevel edges, and the bevel faces between them will form regardless of the configuration of the vertices at the end of the crystal edge because their formation does not depend on any process taking place at the corners. Several such beveled edges can join in a single vertex – thus the geometrical situation can become rather complicated. In addition, even without the presence of any bevel faces, vertices may form one or more truncation faces.

7. TRUE 3D CORNERS

True crystal corners where **all** incident edges are of the **same** type (convex or concave) are relatively easy to analyze. Saddle points offer more challenges and will be discussed in a separate section.

7.1 Vertex Movements

When there are exactly three faces incident on a crystal corner, the three edges between them each move perpendicular to the chords between the tips of the slowness vectors of the respective pairs of faces (Section 2.3). Correspondingly, the vertex, which moves in each of the three planes swept out by the three edges, moves perpendicular to the unique chordal plane through the tips of the three slowness vectors; its speed is the reciprocal value of the length of the normal vector from the vertex to that plane. This fact can also be derived from a 3D analog of Figure 5 in which the sphere that uses the velocity vector of the original corner vertex as a diameter is inverted at a unit sphere around the original vertex position. Such a transformation maps this sphere into the chordal plane mentioned above. This construction of the vertex movement is valid for convex and concave corners as well as for saddle points (Section 8) as long as there are exactly three faces incident on the vertex and as long as there are no truncation faces emerging.

7.2 Vertex Splits

When there are more than three faces present, the tips of the corresponding slowness vectors generally do not lie in a single plane. The vertex figure has to be decomposed into several planar facets by forming the convex hull around the tips of all the slowness vectors. Each corner on this hull will define a new face, while each facet on the hull defines a trajectory for a vertex. The ridges between the facets correspond to newly forming crystal edges. For instance, the four-sided convex pyramid tip in Figure 13b will only survive as a single vertex if all slowness vector tips lie in a single plane. In general, it will split one way (a) or another (c) depending on the relative lengths of these four vectors: the upwards (fast) ridge in the convex hull (Fig.13d,f) is perpendicular to the new edge forming between the two split vertices. In general, in the absence of truncation faces, an n-sided vertex will split into n-2 three-sided subvertices with n-3 new edges between them.

When there are directions with fast etch-rates in the range of orientations of interest at a vertex, *truncation* or *bevel* faces may arise in addition to the splits discussed above. They will show up in the SSS as peaks that are sufficiently high to form corners in the convex hull stretched over the SSS. Extreme values on the bounding arcs of the original vertex figure result in bevel faces along the edges, and extrema in the interior of the vertex figure produce truncation faces. All of the emerging faces can be found by forming the

convex hulls over all minima of the slowness surface for convex crystal corners and over all the maxima for concave corners. The resulting polygonal hulls are the duals of the resulting structure of split vertices and new edges. The normal onto each facet of the hull defines the new vertex trajectories. This construction automatically reflects the complete interplay between all truncation faces and bevel faces.

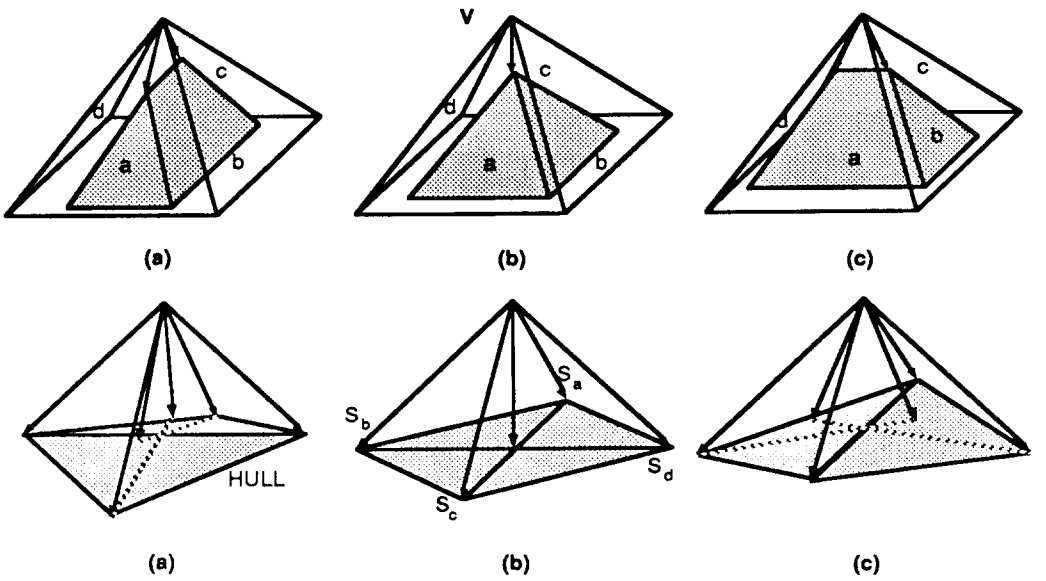

Figure 13: *Etching a multifaced corner will typically split the vertex one way (a) or another (c); only as a special case the vertex will stay intact (b); corresponding slowness surface segments (d,e,f) with face normals producing vertex trajectories.*

7.3 Trees of Future-Edges

Foote [Foot90, p48] employed an alternative method to find the connectivity of the edges forming at a split vertex. He used a recursive processing of the anticipated edge positions some small time increment into the future and then determined the mutual intersections between these *future edges*. To distinguish the actual intersections that appear in the corner geometry from the virtual intersections on the extensions of the edges, this edge structure was processed recursively from the outside inwards.

Whenever two adjacent future edges have their first intersection with each other, they are combined, i.e. the face in between is terminated, and a new edge that is the intersection of the two outer adjacent faces is formed. This process continues until all edges have been connected into a single tree.

If there are truncation faces present, the network formed by the edges must form a graph that contains a loop for each of the emerging truncation faces. Each truncation face is individually inserted into the future-edge tree by intersecting the face plane with all the edges and constructing the appropriate loop [Foot90, p52]. This is obviously a much more involved process than simply forming the dual structure of the appropriate slowness hull.

8. SADDLE CORNERS

A bigger challenge is offered by saddle points where a mix of convex and concave edges come together (Fig.14). Since they are neither purely convex nor purely concave, one does not know whether to use the inner or the outer convex hull to find potential new faces.

8.1 Simplest Saddle Points

Figure 14a depicts two types of simple saddle corners, V and W, with only three faces. In both cases, the vertex trajectory can be easily computed as the normal onto the chordal plane as in the case of a true convex crystal corner.

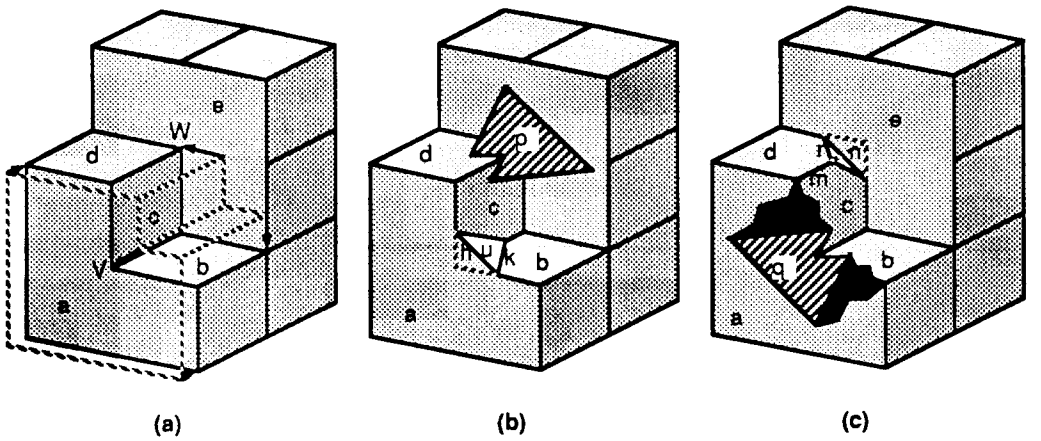

Figure 14: Two types of 3-sided saddle corners: V and W (a). No truncation faces can emerge outside the corner (b) or inside (c).

A natural question is whether it is possible to produce any new truncation faces at such corners. Figures 14b,c show that this is not possible unless some of the edges themselves produce bevel faces. Any truncation face would have to pass the original vertex either outside (Fig.14b) or inside (Fig.14c) the bulk of the saddle corner. The outside face p for corner type W and the inside face q for corner type V, which are both shown striped in Figure 14, are clearly impossible. Without additional bevel faces along two of the original crystal edges, these faces would have two of their edges dangling in space which is impossible for a facet that is part of a boundary of a solid.

The outside face u for corner type V and the inside face r for corner type W, shown white in Figure 14, are geometrically possible but must be ruled out within our first order etching model. For instance, it is not plausible that there could be a mechanism that prevents the atoms along the convex edge h of face u to be removed less quickly than the atoms along the concave edge k between faces b and c (Fig.14b). Similarly, it is implausible that atoms along face e should etch faster than other atoms along the edge m between faces c and d (Fig.14c), so as to produce the notch bounded by face r. In other words, if a fast-etching face with the orientation of r could start in the corner W, the same type of face could start anywhere along edge m, leading to a bevel face along the whole edge. Thus it is concluded that no truncation faces can form on a 3-sided corner that has a mix of concave and convex edges.

8.2 Pseudo Saddle Corners

Figure 12d also shows a corner with convex and concave edges. However, the analysis for this case is the same as that for the filled-out convex corner corresponding to the CCW loop (A, B, I). The CW loop (I, C, D) cannot produce any truncation faces for the same reasons as discussed above.

For these reasons we like to call such vertices pseudo-saddles. They are characterized by the fact that all incident edges and faces fit into a half-space on one side of the corner vertex. The corners V and W in Figure 14 are a limit case of such pseudo-saddles, since their edges and faces also fit into a single half-space.

8.3 Actual Saddle Corners.

Figure 15-1 shows a more interesting saddle corner. In this case there are at least two pairs of convex and concave edges in an alternating sequence. This forms a true saddle corner in which the incident edges do not fit into any half-space. If faces a and c in such a corner move considerably faster than faces b and d, what would be the result ? If we move all four faces in accordance with the assumed etch-rates and then let those four planes intersect one another, we may obtain the geometry shown in Figures 15-2 or 15-3. But how do we know which way the vertex will split, and whether there will be other faces emerging ?

Foote (Foot90, p46) jumps to the conclusion that for reasons similar to the ones above, no new truncation faces can form at any saddle point without the emergence of some bevel faces along the original edges. However, recently an intriguing case has been found where a four-sided saddle corner can produce an isolated truncation face without the presence of any bevel faces (Fig.15-4). This shape can result, if the horizontal face m etches at a rate that is fast compared to the rate of the two slow-etching faces, so that it forces a bevel face at the convex edge between the two slow faces, and if it is simultaneously slow compared to the rate of the two fast-etching faces, so that it forces a bevel face at the concave edge between the two fast faces.

The difficulty in analyzing this situation with Foote's method (Section 7.3) is that because of the pin-wheel configuration of the future edges (Fig.15-1b) there is no single future-edge intersection which is the *first* intersection for both edges. Thus this edge figure cannot readily be simplified from the outside inwards. Depending on the assumed etch-rate distribution (Fig.15-2, 15-3, 15-4), the resulting connectivity of the edges at this corner will indeed be different. Figure 15-2 shows a first situation where we assume that the etch-rate in the vertical direction is slower than any of the etch-rates of the four faces. In this case the central vertex will split in two, forming a convex edge between the slow-etching faces a and c. The corresponding slowness surface segment is a pyramidal concave pit.

Figure 15-3 shows the opposite situation. Here the vertical etch-rate is assumed to be much faster than any of the rates of the four faces. Thus the slowness surface patch is a 4-sided convex pyramid. In this case the vertex will split the opposite way and form a concave edge between the two fast-etching faces.

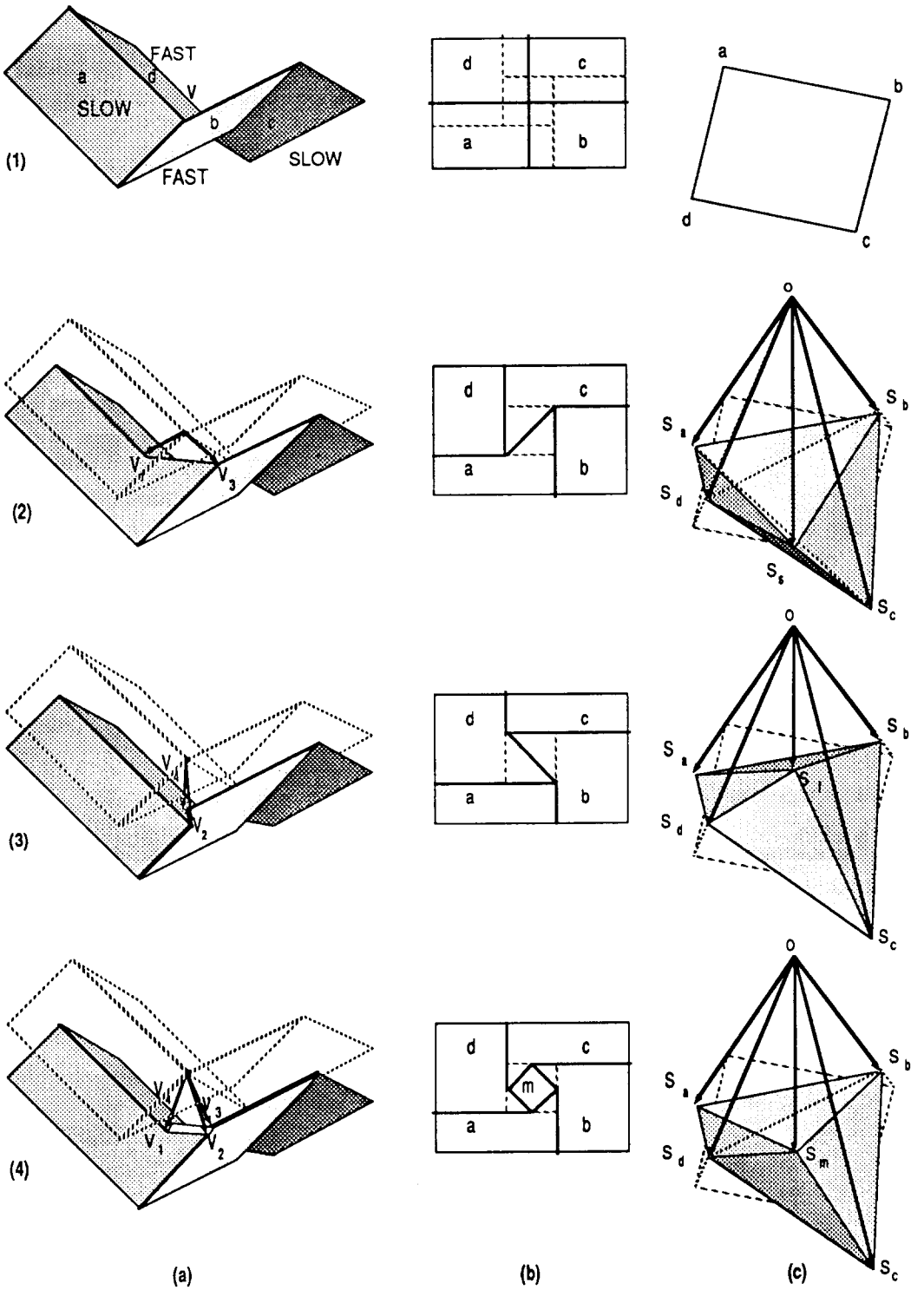

Figure 15: An interesting saddle corner. The crystal shapes before etching (1a) and afterwards (2a), (3a), and (4a); schematic top views of the corresponding faces and future edges (b) and the slowness surface segments (c) for three different etch-rate distributions (2), (3), and (4).

Figure 15-4 shows the interesting intermediate case. Here the vertical etch-rate is of intermediate value, faster than the combined rate of the two slow faces at the convex edge, but slower than the combined rate of the two fast faces at the concave edge. The slowness surface is now itself a saddle surface. The orientations of the four facets in the SSS readily indicate how the vertex V will split. Only in the situation shown in Figure 15-4c are the trajectories of all four subvertices diverging with the proper ordering in space. In cases (2) and (3), two pairs of trajectories do not separate properly but run into one another; thus only a two-way split results. Correspondingly, the simplified hull over the SSS should only show two facets. This is indeed the case if we take the outer convex hull over the four points S_a,... S_d in Figure 15-2c and the inner convex hull in Figure 15-3c. But how do we know which hull to take ? Moreover, Figure 15-4c isn't even a convex hull at all ! How can we generalize this approach if the SSS has many maxima and minima side by side ?

8.4 Non-Dominant Faces Defined by Boundary Constraints

Foote discusses an interesting case of a face that is limited in its growth by a virtual zero-length edge (Foot90, p56). Figure 16a shows a slow bevel face s growing in a concave groove between two faces l and r. This face s forms also a convex edge with the cover face c. If we assume that on this new edge (s,c) there is a fast bevel face f (Fig.16b) that etches so quickly that this edge gets reduced to zero length faster than the widths of bevel S grows, the two edges (l,f) and (r,f) will continue to meet in a point, while the remnants of the fast bevel f continue to strip away part of the slow bevel-volume s (Fig.16c). This continued stripping action will produce a triangular face t that is anchored at the original vertex V_0 and which provides the termination of the bevel s towards face c. The orientation of this face does not correspond directly to one of the extreme points of the slowness surface, since it is defined by the etch-rates of the faces around it. Furthermore, its growth rate is constrained by the rate at which the bevel grows in width.

Foote's simulator cannot represent this face t directly. It models it as a collection of small steps that get emitted by the periodic reevaluation of the situation at the edge (s,b) when it has grown to some threshold length. Since the steady-state geometry depicted in Figure 16c clearly has a dual representation, we should be able to determine that situation directly from a corresponding simplified SSS as in the case of simpler corners.

Figure 16d shows the vertex diagram for the starting situation at vertex V_0. If there is a slowness maximum on the arc between S_l and S_r, the bevel face s will form, and triangulation of the SSS would force an arc between S_c and S_s. The resulting two triangles (Fig.16d) represent the split of the Vertex V_0 into V_1 and V_2 (Fig.16a). If we now further assume that along the arc S_c-S_s there exists a maximum of the etch-rate at some location f, the SSS must be further tessellated into 4 triangles: V_1,... V_4 (Fig.16e). However, if there is a convex ridge between the two triangles representing the trajectories of V_3 and V_4, the face normals occur in the wrong left-to-right order to represent an actual split. This means the subvertices V_3 and V_4 will have to remain together at vertex V_0 and need to be represented by a single planar facet in the SSS. Thus the simplified SSS will have to be truncated by the plane of the original facet representing V_0. The intersection of arc S_f-S_s with this plane determines the location of vertex t (Fig.16f) and thus the orientation of the actual face t emerging at the crystal corner (Fig.16c).

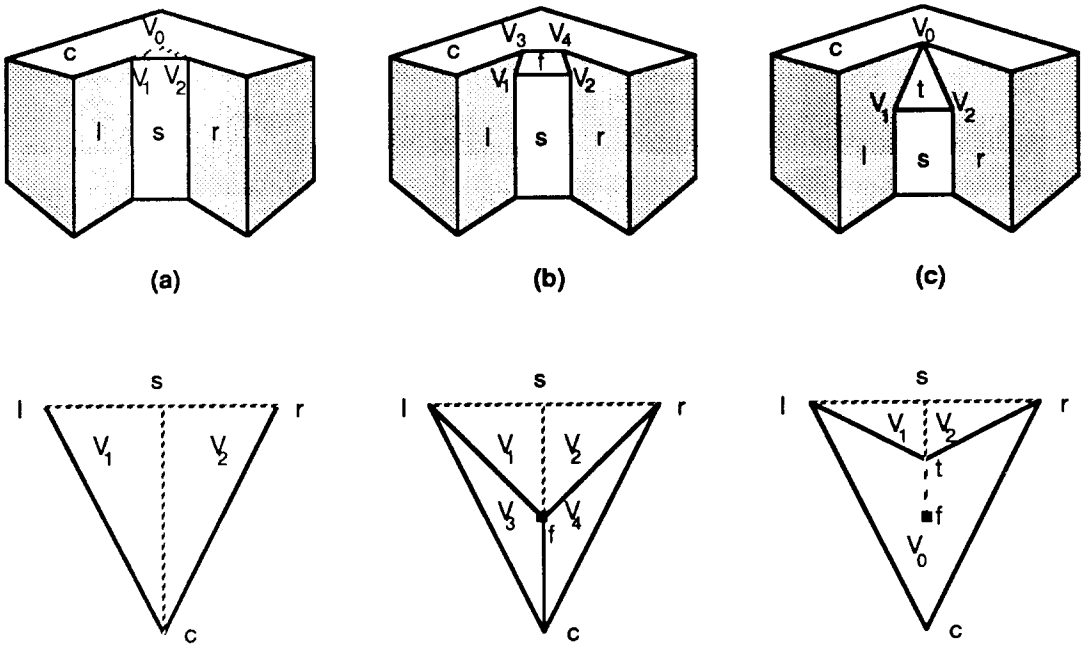

Figure 16: Three different top terminations for bevel face s (a), (b), (c), and the respective vertex diagrams (d), (e), (f).

The last example shows particularly convincingly what can be gained from the analysis of the slowness surface and the construction of the simplified SSS. The whole splitting behavior and the connectivity of all old and new edges can be obtained directly as the dual of the simplified SSS. There is no need for any reevaluation of the subvertices after a split, and the problems with virtual edges of zero length, which Foote solved by introducing an artificial length threshold [Foot90, p57], are completely avoided.

For all the relatively simple cases discussed in this section, it could be made clear what the simplified SSS had to look like to produce the expected results. But how do we find this polyhedral surface for arbitrarily complex corners with an arbitrarily complex slowness surface ?

9. GENERAL CORNER ANALYSIS

The goal of the corner analysis is to determine the trajectory – or trajectories if the corner splits – of each vertex parameterized in time. The key step is to find the emerging new facets and edges and their respective connectivity. We need a reliable program to handle all possible corners.

9.1 True Corners

For true convex and concave corners, we have presented a simple and direct method to find a faceted convex hull over the slowness surface segment (SSS) that is the geometrical dual of the resulting corner structure – including all truncation and bevel faces. The con-

vex hulls used in these cases can be understood as a simplification of the detailed SSS spanned by the given face normal directions of the original crystal corner. In the case of a concave corner, any concave pit in the convex hull of the slowness surface corresponds to a vertex surrounded by a sequence of facets that would have vertex normals that denote virtual splitting subvertices that run into one another rather than diverging properly as would be necessary to produce a splitting vertex with a new face in the middle. Such concave pits are thus culled away by the construction of the convex hull, leaving only true convex vertices that correspond to emerging slow truncation faces at the concave corner.

Similarly, all vertices on the inner convex hull (or concave hull) associated with a true convex corner must be true concave pits in order to represent emerging fast truncation faces. In both cases, the formation of the convex hulls can thus be understood as culling away those features of the SSS that cannot give rise to new emerging faces.

9.2 Saddle Corners

The same principle can now be applied to the SSS associated with a crystalline saddle corner. Saddle corners are characterized by the fact that at least part of their vertex diagram is a loop with reversed (CW) contour direction. For truncation faces to emerge in such a surrounding, it is necessary that the corresponding vertex on the slowness surface be surrounded by facets that have a similar reversed (CW) ordering of their face normals. This means that such vertices themselves must be saddle points such as the vertex m shown in Figure 15-4c.

This leads to the strong conjecture that the simplified slowness hull that represents the dual of the final corner geometry for a saddle corner must be some sort of saddle surface itself which spans the given contour of the SSS and satisfies all constraints along this contour. Any true convex corners or concave pits on the slowness surface would have to be culled away, since they cannot give rise to any truncation faces owing to the incompatible ordering of the associated trajectories of the subvertices.

9.3 A Unified Approach

The above insight leads to the following conceptual construction algorithm for the simplified SSS: Label the set of faces around the crystal corner in CCW order and draw the corresponding vertex diagram onto the lattice of key crystal plane orientations. Analyze each contour segment corresponding to one of the crystal edges incident on the corner being analyzed and construct the proper inner or outer convex piecewise linear path through slowness space which defines the bevel faces. Distinguish three different regions in the vertex diagram: (a) CCW loops corresponding to convex corners, (b) CCW loops corresponding to concave corners, and (c) CW loops corresponding to saddle corners. Within each of these regions, remove all inappropriate features on the SSS and simplify it so that it only contains pure concave vertices in (a), pure convex vertices in (b), and saddle vertices in (c). This will produce the proper inner/outer convex hulls for the true crystal corners and saddle surfaces for regions associated with saddle corners which are all compatible with the constraints already established on the contour of the vertex diagram during edge analysis.

9.4 Efficient SSS Simplification.

For convex hulls, well-known efficient construction algorithms exist. For saddle surfaces this is not the case; it is not even clear whether in general the problem is well defined! However, for our purpose of SSS simplification, we have a more specialized problem. We are **not** trying to construct a saddle surface or a convex hull for an arbitrary set of points. Rather, we try to cull away unwanted features on an already known single-valued, polyhedral surface. This also properly defines the construction task for the saddle surface. An efficient way to construct these simplified slowness surface segments is the subject of current research.

10. A PROTOTYPE SIMULATOR

Prototypes have been constructed of two efficient simulators based on a polygonal boundary representation of the crystal surface. A complete simulator for the two-dimensional case has been built which takes arbitrary biclinic etch-rate diagrams and accepts initial crystal geometries of arbitrary complexity. For the first implementation of a three-dimensional simulator [Foot90, p60], two simplifications have been introduced: First, the slowness diagram is approximated with a piecewise planar triangulated surface. Second, only local interactions between faces are being considered so far. Topology changes resulting from holes etching through to the other side of the wafer have not yet been implemented. In this simulator, the modeling of the etching process in our surface-based three-dimensional simulator happens in several discrete phases.

10.1 Constructing a Complete Slowness Diagram

First, the user must provide enough data to specify a complete etch-rate diagram. Whether the information about the etch-rates in key directions is obtained from the literature or from a polar diagram generator [Foot90, p31], these values are entered into an etch-rate data file. The user needs to enter explicitly the values for a generic key direction of the crystalline material under consideration, the program figures out by itself the values for the symmetrical directions. The complete 4π shell of the slowness diagram is then approximated with a triangulated surface supported by the values for the key directions. The extrema on this surface, among others, specify the potential face orientations in which new faces might emerge.

10.2 Corner Geometry Analysis

For each corner currently present in the crystal shape being etched, the infinite set of all possible surface orientations is reduced to those orientations corresponding to faces that will actually grow in size. This analysis is currently based on the convex hull method described in Section 7.

To prevent the data structure from growing more complex than necessary, the program removes the elements that have disappeared from the boundary of the etched shape. For instance, edges that have shrunk to zero length are eliminated, their end vertices merged, and the attached edges properly re-linked. Implementation problems arise here from coplanar face elements that fold back onto themselves and from bevel faces that shrink to zero width.

For applications in microfabrication, the simulator must support masking of the crystal structure. This is implemented by introducing appropriate special cases in the various algorithms. For instance, at an edge between two masked faces, the geometry will remain unchanged, and thus the computation of the candidate list can be omitted. At an edge between a masked face and an unmasked one, overhangs will form owing to undercutting. If such virtual overhangs are introduced along all mask edges and if the orientations of the new faces are properly chosen, then the correct geometry changes at the vertices along the mask's boundaries will emerge almost automatically.

10.3 Offset Surface Construction

All geometry changes are captured in the calculated vertex trajectories through space. With these trajectories suitably parameterized in etching-time, the new crystal contour (2D) or surface (3D) for a specified instant in time can then be constructed readily. The vertex coordinates are calculated for the desired time point. The corresponding planar crystal facets are extracted from the boundary representation and are sent to the display. The display process is so fast, that once the vertex trajectories have been calculated, real-time interactive animation of the etching process is possible.

10.4 Planned Revisions and Enhancements

We are in the process of revising parts of the simulator. In particular, we hope that the introduction of a unified corner analysis based on the simplified slowness surface segments will make the code simpler and more robust and will handle saddle corners and non-dominant faces defined by boundary constraints in all circumstances without the need to introduce special cases.

Another required enhancement of our current program is to handle non-local interactions. Since the topology of the contour can change, we need to predict where vertex trajectories run into one another or into other faces. With this goal, we formulate the etching simulation as an event-driven process where the relevant events are the intersections of trajectories that may lead to topological changes. The expected etching-time at which these intersections would occur are calculated, and a corresponding event is placed onto the event queue. The topology update for the new offset surface is completed for the earliest etching time appearing in the event queue. Any such update may change the structure and may introduce new events into the queue. For any new corners created, its candidate faces must be examined and new faces introduced into the contour. This processing continues until there are no more topology-driven events on the queue with time stamps earlier than the etching termination time specified by the user.

Construction of a complete simulator for three-dimensional shapes, with capabilities equivalent to those of our 2D simulator, requires no additional conceptual breakthroughs, but a fair amount of careful software engineering. There also is an important issue of efficiency. It is impractical to intersect all vertex trajectories with all other faces to predict where topologically significant intersections might occur. Some efficient space management scheme, such as a grid or an octal tree, has to be employed to keep the necessary tests from growing with the square of the number of all the facets in the etched structure.

11. 3-D SIMULATION RESULTS

Here we present some results obtained with our simulator to demonstrate the important role that emerging truncation and bevel faces play in anisotropic crystal etching. A representative set of etch-rates for a simple cubic lattice with a hypothetical anisotropic etching process is shown in Table 1 [Foot90, p38]. This is the basis for the simulations described in this section. The full slowness diagram is generated through interpolation. While such a diagram may not represent any actual material, its consistency should at least allow us to carry out meaningful experiments with our surface-based etching simulator.

Table 1: Key Etch-rates Derived from a Simple Cubic Lattice

Face Orientation	Etch-rate	Slowness	Relative Slowness
{2 2 1}	.0017	588	1.0
{2 1 1}	.0014	714	1.2
{1 1 1}	.00058	1724	2.9
{2 1 0}	.00046	2174	3.7
{1 1 0}	.00030	3333	5.6
{1 0 0}	.00003	33333	56.0

In the long run it may even be possible to use the atomistic etch-rate modeling approach used to generate Table 1 to flesh out in a consistent manner partial experimental etch-rate data into a complete 4π slowness diagram. This can possibly be achieved by adjusting the six to eight parameters that describe the bond-strengths in the model so as to match the etch-rate data for the directions in which it is known. However, we have not yet investigated how easy it would be to carry out such a matching.

Figure 19 shows some representative results obtained with the three-dimensional simulator. The starting crystal has the shape of three intersecting bricks. A simple cubic crystal lattice is assumed with the etch-rates listed in Table 1. If the brick faces are aligned with the lattice planes, anisotropic etching will develop the faceting shown in Figure 17.

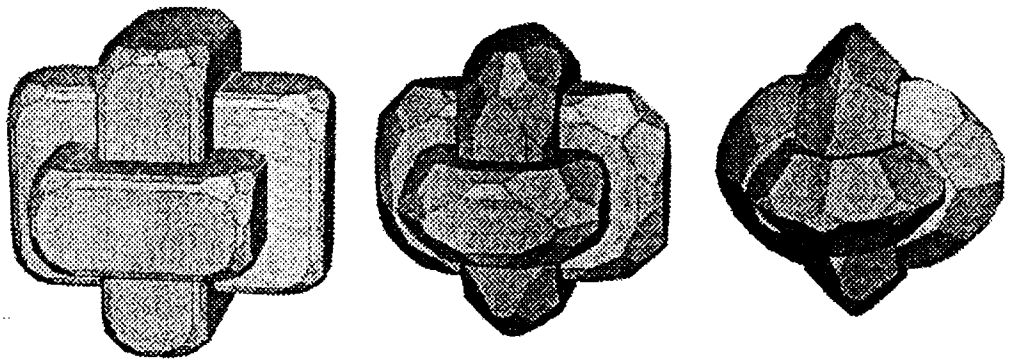

(a) (b) (c)

Figure 17: Etching a crystal shape for three different time durations (a), (b), (c).

However, if the initial shape is at some odd angle with respect to the underlying crystal lattice, the faceting becomes more complicated and irregular, and many intriguing bevel edges develop at the concave edges (Fig.18a). Figure 18b gives a close-up view of one of the concave corners. For more examples see [Foot90].

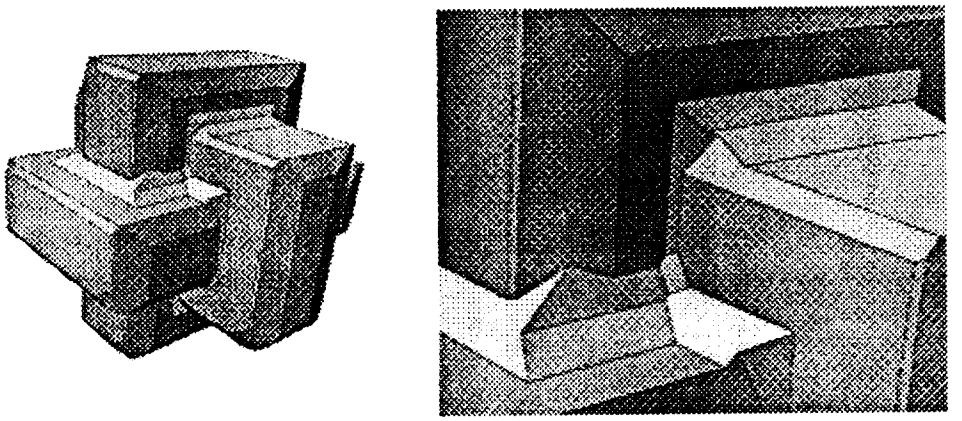

(a) (b)

Figure 18: Etching of the shape of Fig.17 with a different crystal orientation (a); close-up of a concave corner (b).

12. CONCLUSIONS

Considerable insight has been gained into the etching behavior of uniform but anisotropically etching polyhedral objects. In particular, we believe that we now understand precisely under what circumstances bevel faces or truncation faces can form at crystal edges or corners. The role of the slowness surface has been elucidated, and a unified corner analysis method based on simplified hulls over relevant segments of this surface has been conceived. However, this new method has not yet been implemented and must clearly be subjected to more scrutiny.

Prototypes have been constructed of two efficient simulators based on a polygonal boundary representation of the crystal surface. They demonstrate the viability of the approach. The same data structure, algorithms, and overall analysis can also be used to model growth or deposition processes: in this case the surfaces move outwards. Even processes such as the diffusion of impurities or oxidation processes can be modeled with a boundary representation. In the latter case, two surfaces need to be moved simultaneously, one inward and the other outward.

Modeling the etching (or other processing) of a crystalline substance through the movement of a few hundred polygons is very efficient. Since a surface-based process simulator can compute a new crystal surface in seconds, it makes a handy tool for interactive exploration of microfabrication process sequences.

13. ACKNOWLEDGMENTS

Many thanks go to Bill Foote who developed the initial prototype simulation programs. Readers who want more detailed information should ask for his Masters report [Foot90]. We would like to thank Siemens AG and the Semiconductor Research Corporation for their support of our modeling efforts.

14. REFERENCES

[BFMS73] D. J. Barber, F. C. Frank, M. Moss, J. W. Steeds, I. S. T. Tsong, "Prediction of Ion-bombarded Surface Topographies Using Frank's Kinematic Theory of Crystal Dissolution," J. of Materials Science, Vol.8, pp 1030-1040, (1973).

[Bass78] E. Bassous, "Fabrication of Novel Three-Dimensional Microstructures by the Anisotropic Etching of (100) and (110) Silicon," IEEE Trans. ED-25, No.10, pp 1178-1185, (1978).

[Bean78] K. Bean, "Anisotropic Etching of Silicon," IEEE Trans. ED-25, No.10, pp 1185-1193, (1978).

[Foot90] W. F. Foote, "Modeling of Anisotropic Crystal Etching," Technical Report #UCB/CSD 90/595, Computer Science Division, U.C. Berkeley, (1990).

[Fran58] F. C. Frank, "On the Kinematic Theory of Crystal Growth and Dissolution Processes," in "Growth and Perfection of Crystals," Wiley and Sons, New York, pp 411-419, (1958).

[Lee69] D. B. Lee, "Anisotropic Etching of Silicon," J. of Applied Physics, Vol.40, No.11, pp 4569-4574, (1969).

[Pete82] K. E. Petersen, "Silicon as a Mechanical Material," Proc. of the IEEE, Vol.70, No.5, pp 420-457, (1982).

[SaKT89] K. Sato, A. Koide, and S. Tanaka, "Measurement of anisotropic etching rate of single crystal silicon to the complete orientation," JIEE Symposium on Micromachining and Micromechatronics, Univ. of Tokyo, Oct. 27, pp 19-27,(1989).

[SeCs82] H. Seidel and L. Csepregi, "Studies on the anisotropy and selectivity of etchants used for the fabrication of stress-free structures," 1982 Spring Meeting, Electrochemical Society, Montreal, Canada, Abstract No. 123, pp 194-195, (1982).

[Séqu91] C. H. Séquin, "Computer Simulation of Anisotropic Crystal Etching," Digest of Papers, Transducers'91, San Francisco, pp 801-806, (1991).

[SéSm90] C. H. Séquin and K. Smith, "Introduction to the UniGrafix Tools 3.0" Technical Report #UCB/CSD 90/606, Computer Science Division, U.C. Berkeley, (1990).

[Weir75] D. F. Weirauch, "Correlation of the anisotropic etching of single-crystal silicon spheres and wafers," J. of Applied Physics, Vol.46, No.4, pp 1478-1483, (1975).